Effect of the interfacial electric field on the HER on Pt(111) modified with iron adatoms in alkaline media

Francisco J. Sarabia, Victor Climent[*], and Juan M. Feliu*[**]

Instituto Universitario de Electroquímica, Universidad de Alicante, Carretera San Vicente del Raspeig s/n, E-03690 San Vicente del Raspeig, Alicante, Spain

Cover Text:

The study of the hydrogen evolution reaction on iron modified Pt(111) single crystal surfaces provides new clues to the understanding of the parameters that govern the rate of this reaction. Information from measurements using the laser induced temperature jump experiments allows to stablish relationships between the interfacial electric field, the polarization of interfacial water molecules and the rate of H_2 production.

Abstract

The study of the hydrogen evolution reaction (HER) aimed to reach a deeper understanding of the parameters that control the rate of this reaction is of great importance given the technical relevance of hydrogen production as an energy vector in the so-called hydrogen economy. In previous works, laser-induced temperature jump (LITJ) experiments on Pt(111) modified with $Ni(OH)_2$ in alkaline media have revealed the importance of the interfacial electric field in the rate of the HER. It was hypothesised that small amounts of $Ni(OH)_2$ cause a decrease of the electric field because of a negative shift of the pzfc toward the onset of the hydrogen evolution. In this work, to test the validity of this hypothesis, the study has been extended to Pt(111) surfaces modified with $Fe(OH)_2$ .The modified surfaces have been studied voltammetrically, and the voltammetric charges have been analysed. The voltammograms show a peak in the hydrogen evolution region that suggest the transformation in the adlayer from Fe(II) to Fe(0). In agreement with the coulometric analysis, the voltammetric features in the OH adsorption region would be related with the oxidation to the +3 valence state. The results

obtained with LITJ method reflect the existence of a strong interaction of the Fe oxophilic species with the water molecules, shifting the potential of maximum entropy away from the onset of the HER. Hence, the most catalytic surface is the one with the lowest Fe coverage.

Keywords: Hydrogen evolution reaction, iron adatoms, platinum single crystal, Pt(111), laser induced temperature jump, interfacial electric field, potential of zero charge

Corresponding authors:

*Victor Climent: victor.climent@ua.es

**Juan M. Feliu: juan.feliu@ua.es

1 Introduction

The HER is one of the most studied reactions in electrochemistry. The study of this reaction has received renewed interest in last decades given the potential use of hydrogen as an energy carrier, being possibly the most promising solution to meet the large energy demand without compromising the quality of the environment.[1] This idea has promoted the posibility of developing an economic-energetic model called the hydrogen economy.[2] For this reason, the study of the enhancement in the catalytic activity towards this reaction presents great importance nowadays. In some works, different materials such as sulphides[3], metal alloys or combinations of metals [4] have been tested for the HER following a trial-and-error methodology. Other studies have focused on relating the physico-chemical properties of the electrode material with the kinetic parameters of the HER. In this regard, studies carried out by Trasatti revealed the application of the Sabatier principle to the HER, and hence, the hydrogen binding energy (HBE) as a descriptor for this reaction.[5] By using ultra-high vacuum techniques (UHV), Zerdjanin et al. proposed the work function as another descriptor for the HER.[6] Besides those physico-chemical properties of the electrode material, there are other important parameters such as the reaction media and the existence of intermolecular interactions between the different components of the interphase. In this regards, it has been reported that the nature of the cation enhances the HER on Pt and Pt/Ni in alkaline media ($Li^+ > Na^+ > K^+$).[7] In addition, it has also been observed that the presence of oxophilic species such as d-metal oxides on Pt(111) in alkaline media improves the rate of the HER.[7a] The explanation for this enhancement was based in a bifunctional model where the only important parameter considered was the OH-binding energy from the adsorbed species to the d-metal.[7a, 8]

Other more recent idea proposed by Koper et al, considers the role of the interfacial electric field in the HER and its effect on water polarization.[9] This idea is based on the observation of higher rate for the HER on Pt(111) in acid media where the potential of zero free charge/ potential of maximum entropy (pzfc/pme) is close to the onset of the reaction facilitating the proton transfer though the double layer as a consequence of a less rigid water network structure. Conversely, in alkaline media the pzfc/pme lies in a potential region farther away from the onset of the HER, resulting in a more rigid water layer and a more difficult OH^- transfer. The consequence of this effect is a much higher rate of HER in acid than in alkaline media. In relation to this, it was observed that the

nickel presence on Pt(111) in alkaline media shifts the pzfc toward lower potentials, decreasing the interfacial electric field resulting in an increase of the rate of the HER.[9-10] This work presents an interfacial study similar to previous works with nickel in alkaline media but, in this case, the Pt(111) surface is modified with iron adatoms. Coulometric relationships are deduced from the voltammetric charges and the relation between the interfacial electric field with the catalytic activity of the HER for different iron coverages is studied.

2 Experimental

2.1 Chemicals

All solutions were prepared using ultrpure water from an Elga PURELAB Ultra Analytic system (resistivity 18.2 MΩ cm). NaOH solutions (0.1M) were prepared using sodium hydroxide monohydrated (Merck Suprapur). $Fe(OH)_2$ deposits were carried out at open circuit potential by holding the Pt(111) electrode into a 10^{-4}M iron (II) perchlorate (Aldrich 98%) solution during different times. Solutions were deaerated by bubbling Ar for at least 15 min before starting each experiment. During the experiments, an Ar blanket was maintained above the solution to prevent the entrance of O_2 into the cell. The pH of the solutions was measured using a pH-basic-20 pH-meter from Crison coupled with a pH-probe pH 50 12 HACH model.

2.2 Electrochemical experiments

The experiments were performed in a classical three electrode cell configuration using a Luggin capillary to separate the reference electrode from the main working solution at room temperature. Working electrodes were obtained by the method described by Clavilier et al.[11] A platinum wire was used as counter electrode and a reversible hydrogen electrode (RHE) and a Pd-H_2 electrode as reference for the cyclic voltammetry and laser temperature jump method, respectively. Before each experiment, the working electrode was flame annealed in a propane-oxygen flame and cooled in a hydrogen/argon (1:3) atmosphere.[12] Afterwards, the electrode was protected by a drop of ultra-pure water saturated with these gases prior to being transferred to the cell or to carry out the iron hydroxide deposition. The working electrode was contacted with the solution in the

hanging meniscus configuration. The cyclic voltammetries were performed using a potentiostat (eDAQ EA161) connected with a signal generator (PAR 173) and a digital recorder (eDAQ, ED401).

2.3 Laser-Induced Temperature Jump Method

In order to perform the laser-induced jump temperature experiments, a system with a fourth electrode is employed in addition to those typically used in a conventional electrochemical system (counter, reference and working electrode). This fourth electrode is polarized at the same potential as the working electrode so the potential difference between both electrodes is measured when the thermal perturbation is produced once the laser strikes the surface of the working electrode. Approximately, 200μs before firing the laser, the working electrode is disconnected from the potentiostat, leaving the system at open circuit potential. Between successive laser pulses, the working electrode is reconnected to ensure that the potential is kept at the desired value. In this way, the electrode potential change due to the temperature increment is recorded under coulostatics conditions. Each experiment is repeated with a frequency of 10 Hz to ensure that the temperature relaxes to the initial value between measurements. Either 128 or 256 potential transients are recorded and averaged using a Tektronix Model TDS 3054B oscilloscope.

A light source Billiant Q-switched Nd:YAG laser (Quantel) was employed to send out laser pulses of 5 ns with a wavelength of 532 nm. On the other side, a system of convergent and divergent lenses was used to regulate the diameter of the laser beam (4 mm). The energy density of the laser beam was reduced to less than 8 mJ/cm^2 by combining the effect of an attenuator from Newport Corporation (Model M-935-10) and the regulation of the Q-switch time. The laser energy was measured with a piroelectric sensor head (Model M-935-10).

3 Results and discussion

3.1 Voltammetric results

3.1.1 Iron hydroxide deposits

The cyclic voltammetries of the Pt(111) surface with different $Fe(OH)_2$ coverages in 0.1M NaOH are shown in Figure 1 Each iron coverage was obtained by immersing the

Pt(111) electrode in an aqueous solution of 10^{-4}M $Fe(ClO_4)_2$ for a specific time (35s, 60s, and 3min as indicated in Figure 1). As the voltammetric profiles show, when the iron coverage increases, the charge involved in the hydrogen UPD region (0.06-0.4) decreases (Coverages indicated in the figures are calculated using equation (2) and the conclusions of the coulometric analysis described below). In the same way, the peak related to the OH adsorption-desorption centered at 0.77 V decreases while new anodic and cathodic peaks appear at 0.67 V and 0.57 V, respectively. This is similar to what was observed in previous works for nickel adatoms on the same surface.[7a, 8, 10] Even though the origin of the peak centered at 0.67 V is not clear, Subbaraman et al. claimed that this peak corresponds to the enhanced oxidative adsorption of OH ions due to the high oxophilicity of the iron species adsorbed on the surface.[8] X-ray adsorption spectrum (XAS) measurements revealed that iron species adsorbed on Pt(111) form a mixture of Fe(II) and Fe(III) oxides and hydroxides in the HER potential region (below 0 V) and change their oxidation state with the potential becomig Fe(III) in the OER potential region around 1.4 V.[8] On the other hand, as Subbaraman et al. pointed, the Pourbaix diagram for solid iron species also predicts the presence of $Fe(OH)_2$ and Fe_3O_4 in alkaline media at potentials close to 0 V for aerated and non-aerated solutions, respectively. However, these two species ($Fe(OH)_2$ and Fe_3O_4) undergo a change in their oxidation state to +3, above 0.27 V and 0.18 V respectively.[13] In addition, below -0.1 V, iron hydoxides and oxides transform into the 0 valence state.[13] One should bear in mind that the behaviour of surface processes is different from the behaviour of solution processes because the electronic properties of the adlayer are affected by the interaction with the substrate. Therefore, we cannot expect to observe the same iron species predicted in the Pourbaix diagram at the same potentials. Despite the fact that previous works reflect that there could exist a minimum change in the oxidation state for iron between the hydrogen and the OH adsorption-desorption region, the analysis of the charge involved under the peaks of the voltammograms (shown below) points toward a notable change in the oxidation state of the iron adsorbed species. In addition, the observation of cathodic and anodic peaks around -0.2 and -0.13 V respectively, during the HER (see below in Figure 8) suggest that the change from the oxidation state of 2 to the zero valence state takes place at lower potentials.

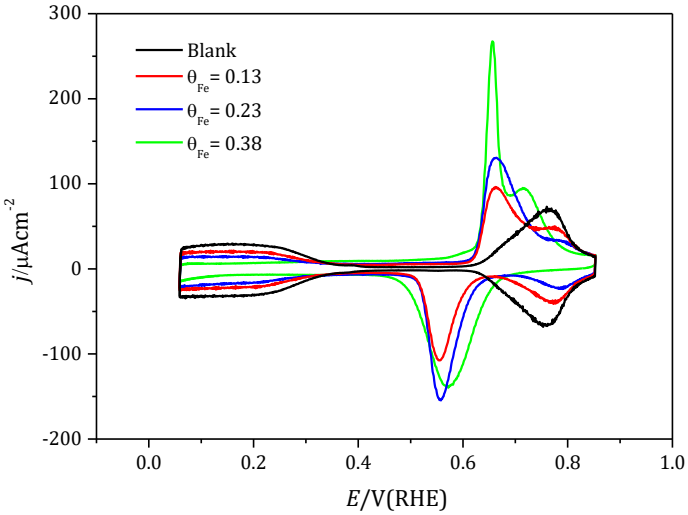

Figure 1. Cyclic voltammograms of the Pt(111) surface modified with different $Fe(OH)_2$ coverages. Scan rate 50 mV/s. 0.1M NaOH. Each one of these coverages 0.13, 0.23 and 0.38 were carried out after holding the working electrode under open circuit conditions during 35s, 60s, and 3min respectively in an aqueous solution of 10^{-4}M $Fe(ClO_4)_2$. Coverage is calculated according to equation (2).

While the CV of the platinum modified with a low iron coverage is stable from the first cycle, it is worth mentioning that this is not the case with the highest coverage registered here. As Figure 2 shows, as the number of cycles increases, the charge corresponding to the OH adsorption-desorption region increases while the charge redistributes between different adsorption states. The peak centered at 0.7 V in the OH adsorption region decreases while a new one appears at 0.66 V. One explanation for this behavior could be that a disaggregation of initial patches with more than one layer takes place, leading to the formation of a more regular and flat adlayer, therefore increasing the active area for the OH adsorption.

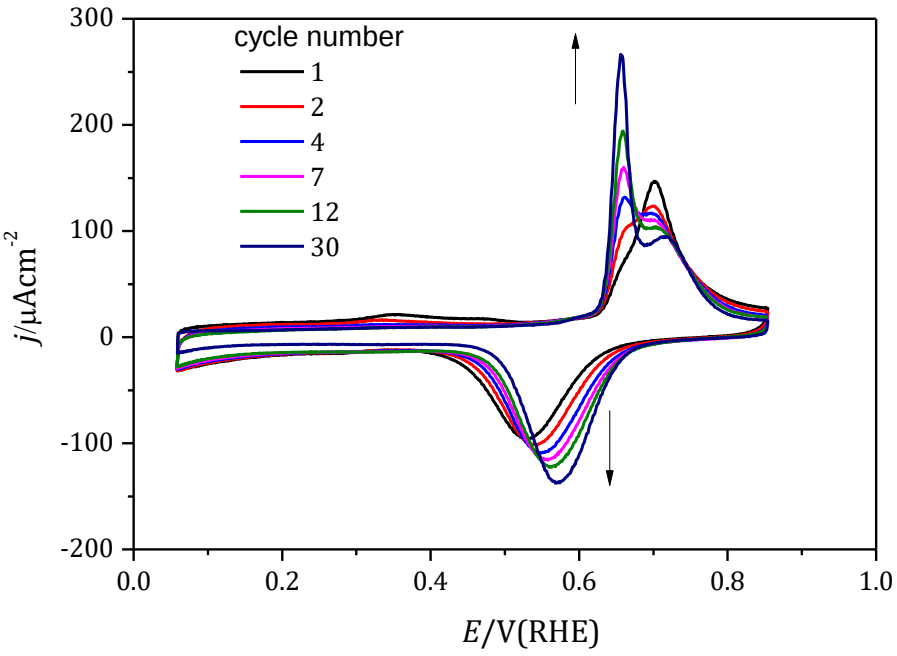

Figure 2. Evolution with the number of cycles of the voltammetric profile for the highest iron coverage. Scan rate 50 mV/s. 0.1M NaOH.

Number of cycle	Charge (μC/cm^2)
1	246
2	248
4	264
7	269
12	280
30	288

Table 1. Average charge obtained from the anodic and cathodic peaks for each number of cycle from Figure 2.

In order to obtain more information about the interface such as the charge distribution and the type of species adsorbed on the electrode surface, the CO displacement technique was employed. For that, the holding potentials were selected at 0.1 V and 0.25 V (Figures 3A and 5A, respectively). During the CO displacement at 0.1 V for the unmodified Pt(111) surface, a positive transient current is recorded as a consequence of the hydrogen desorption with a charge value of 130 $\mu C/cm^2$ (similar to previously reported results).[10] However, this charge decreases with increasing the iron amount even becoming zero for the highest coverage due to the lower availability of free sites for hydrogen adsorption. None of the transients contains negative contributions, that could indicate the presence of species other than hydrogen adsorbed on the platinum sites. The values of the hydrogen charge obtained during the CO displacement are comparable to the voltammetric charge involved in the hydrogen region from the CVs in Figure 1. The values of the CO displaced charge are slightly smaller than the voltammetric charges. This might be due to the small capacitive charge remaining on the CO covered surface.[14] We should also take into account that the small voltammetric charge between 0.06 V and 0.1 V is not displaced in the CO experiment performed at 0.1 V. Similar experiments performed with nickel covered surfaces revealed the existence of negative contributions attributed to displacement of OH species. The fact that no negative contribution is observed with the iron modified surface, suggests that there is a greater bond strength between the OH and the adsorbed iron[10] or a weaker interaction between the CO molecule and the iron adatoms. Figure 3B shows the corresponding CO stripping curves after each one of the CO displacements. On the platinum unmodified surface, CO oxidation appears as a peak at 0.77 V and a broad pre-peak at around 0.60 V with an onset at 0.33 V. The main peak at 0.77 V completely disappears when the surface is covered with iron. In addition, the pre-wave displaces to lower potentials and its charge decreases but never reaching the low potentials registered for the shoulder appearing at 0.33 V in the blank. Therefore, this shows that there is no enhancement in the catalytic activity for the oxidation of CO.

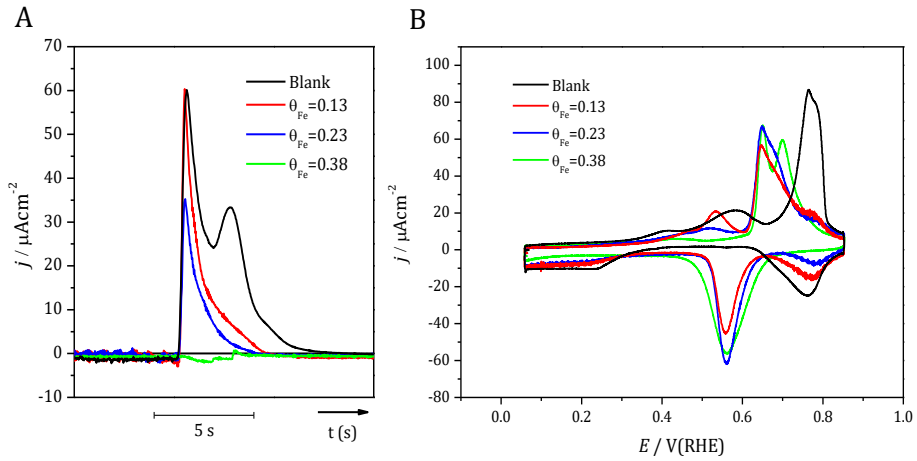

Figure 3. CO charge displacement curves for different iron coverages registered at 0.1 V (A) and their respective CO stripping recorded at 20 mV/s (B). Supporting electrolyte: 0.1 M NaOH

It is worth to highlight that after the CO stripping when the displacement is carried out at 0.1V, the recorded CV is almost identical to the initial one, as it is shown in Figure 4.

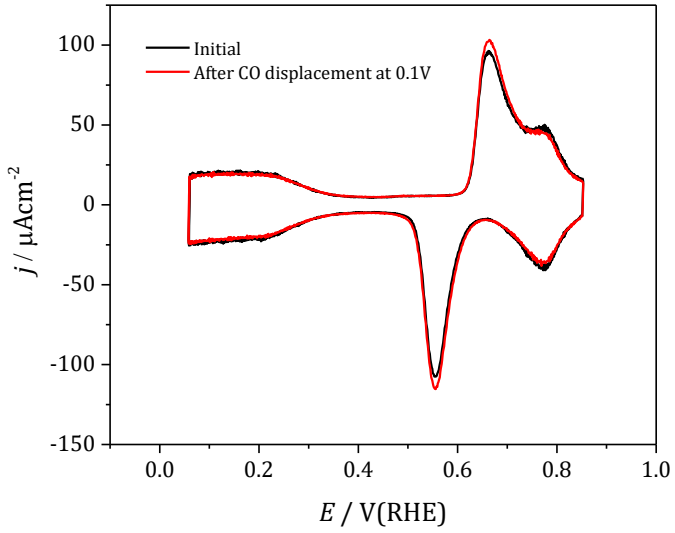

Figure 4. Cyclic voltammogram for the Pt(111) modified with iron ($\theta_{Fe} = 0.13$ has been chosen as representative) before and after the CO stripping after the CO displacement at 0.1 V. Scan rate 50 mV/s. Supporting electrolyte: 0.1 M NaOH

CO displacement measurements at 0.25 V (only shown for Pt(111) immersed in 10^{-4}M $Fe(ClO_4)_2$ during 35s) were also performed. These experiments were done with the hope that, at higher potentials, the Pt-Fe bond would be weaker and the CO might be able to

displace the adatom from the electrode surface to obtain a transient current associated directly to the adsorbed iron species. The results are shown in Figure 5A. However, the CO charge displacement curves only show the charge of the remaining hydrogen adsorbed on the free sites at this potential (full red line and dashed violet line for modified and bare Pt(111) respectively). CO stripping reflects that the CO oxidation curves with and without iron are more similar between them than when the displacement is performed at 0.1 V. As can be seen in Figure 5B, for this case the same peak centered at 0.77 V is observed as in the blank. In addition, after the CO oxidation, nearly the same cyclic voltammogram as for the free Pt(111) surface is recovered (Figure 6). The only remaining signs of the presence of iron are a shoulder at the onset of the OH adsorption and a peak associated to a reduction current, observed at 0.68 V and 0.55 V, respectively. This couple of peaks signals a small remaining amount of iron adsorbed on the surface. Therefore, this suggests that iron adatoms are displaced during the CO adsorption at this higher potential.

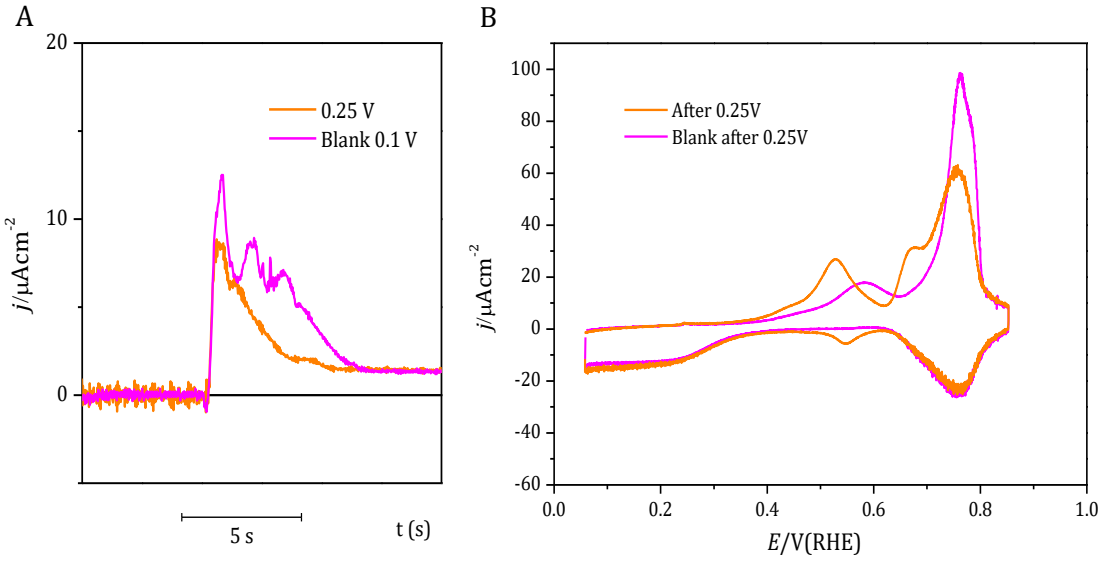

Figure 5. CO charge displacement curves registered at 0.25 V for free Pt(111) and modified holding the electrode in 10^{-4}M $Fe(ClO_4)_2$ during 35s (A) and their respective CO stripping recorded at 20 mV/s (B). Supporting electrolyte: 0.1 M NaOH

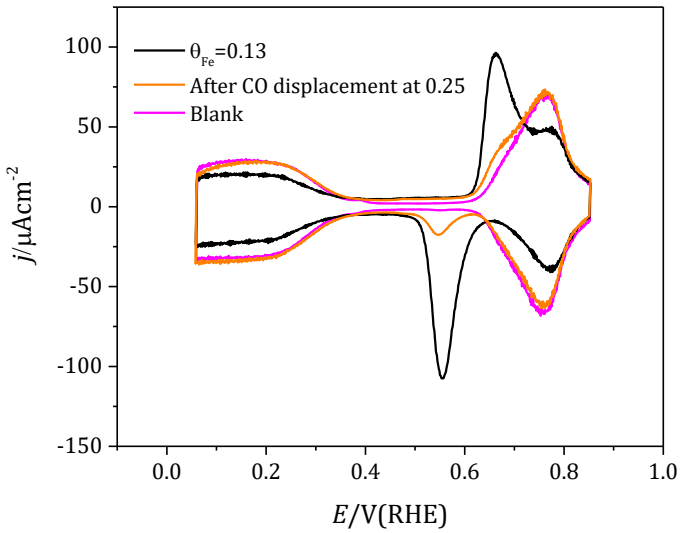

Figure 6. Cyclic voltammogram recorded after CO stripping and CO displacement at 0.25 V for the Pt(111) surface modified holding the electrode in 10^{-4}M $Fe(ClO_4)_2$ during 35s. Scan rate 50 mV/s. Supporting electrolyte: 0.1 M NaOH

3.1.2 Hydrogen evolution reaction

Figure 7A shows the HER at different iron coverages. As can be observed in figure 3, the catalytic activity for this reaction decreases as the iron coverage increases. This result is completely opposite to the one observed in previous works for the Pt(111) surface modified with $Ni(OH)_2$ where the HER rate is enhanced with the increasing nickel coverage.[10] In this case, the onset of the reaction shifts toward more positive potential with decreasing the amount of iron on the surface. Analysis of Tafel slopes provide further information about the activity of the modified surface. For the blank and for iron coverages up to 0.1, Tafel slopes are very similar (ca. 118 mV/dec) and consistent with the one obtained in previous works in alkaline media.[9, 15]. For the lowest Fe coverage, the one that is more electroactive, a lower Tafel slope is also observed. In this case, the electrode was immersed in the $Fe(ClO_4)_3$ solution for just between 2 and 3 seconds and was immediately rinsed with water. Conversely, for the highest coverage, the Tafel slope

slightly increases, becoming less favourable from the electrocatalytic point of view. This change of Tafel slope could be indicating a change in the relative importance of the different steps that conform the mechanism of the reaction as the iron coverage increases. Tafel slope analysis has been developed elsewhere.[16] It has been reported that Tafel slope of 120, 40 and 30 mV/dec are obtained for the Volmer, Heyrovsky and Tafel steps as the rate determining step respectively. Therefore, the Tafel slopes for the low iron coverage are consistent with the Volmer step limiting the reaction rate. The decrease of Tafel slope for the lowest iron amount could suggests a mechanism in which the first electron transfer (Volmer step) has lower effect on the global rate of the reaction. However, for the higher coverages, a change of slope is observed at higher overpotentials, leading to a crossing of the curves, resulting in a higher current for the modified surfaces. These results could be indicating that hydrogen adsorbs in the upd region and low overpotentials with increasing difficulty as the iron coverage increases but once a specific overpotential is reached, in the HER region, the hydrogen adsorption rate is faster. This phenomenon is observed more clearly in figure 8 for the highest iron coverage where there is faster slope increase for potentials below -0.23 V (green curve) in comparison with the curves (blue and red) corresponding to lower coverages. This figure also shows a redox couple overlapped with the HER which can be interpreted as the conversion from Fe(II) to Fe(0) in the negative scan at -0.2 V and the corresponding oxidation in the positive scan from Fe(0) to Fe(II) at -0.13 V.

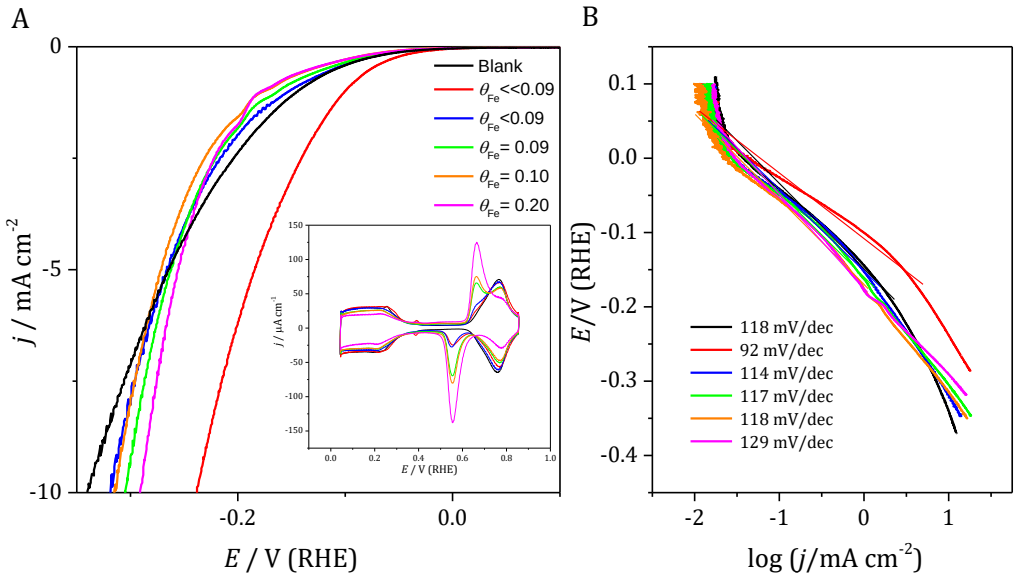

Figure 7. HER of the Pt(111) modified with different iron coverages at 20 mV/s in alkaline media (0.1M NaOH) (A) and their respective Tafel plots (B). Tafel slopes measured in the linear region are indicated in figure B. Coverages are calculated according to equation (2), except for the curve with $\theta_{Fe} = 0.09$, where the coverage was estimated from the hydrogen charge, according to equation (1). For the green and blue curves, the coverage is so low that cannot be estimated according to voltammetric measurements.

It is worth noting that the Tafel slopes were calculated from negative scan before arriving to the cathodic peak in order to obtain the value associated to iron in the 2+ oxidation state. An important observation regarding the redox couple overlapped with the HER is the apparently higher charge in the reduction peak as compared with the oxidation peak. This could be caused by a change of activity towards HER as the redox state of iron changes from (II) to (0). This could indicate a loss of catalytic activity when the iron is in the 0 state, evidencing in this way, that the hydroxide acts as better catalyst for the HER.

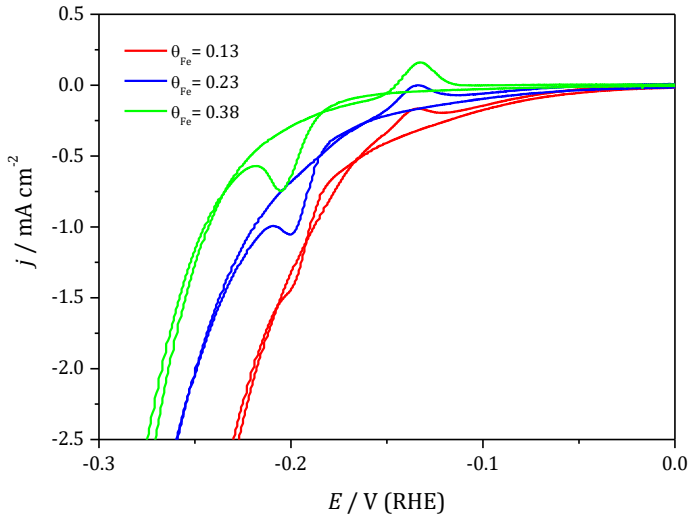

Figure 8. Redox couple appearing during the HER in alkaline media (0.1 M NaOH) of the Pt(111) surface modified with different iron amounts at 20 mV/s.

3.2 Coulometric analysis

In order to obtain information about the iron coverage (θ_{Fe}), and the stoichiometric relationships between different reactions, a coulometric analysis was performed. For that, on one side, the resulting charge from the anodic peak centered at -0.13 V was related with the involved charge in the OH and hydrogen adsorption-desorption region. On the other hand, a relationship between the hydrogen charge and the OH charge was also sought.

Table 2 shows the charges for the peaks appearing at -0.2 V and at -0.13 V during the HER ascribed to the reduction and oxidation of the adsorbed iron specie, respectively (Figure 8). As can be seen in this table, the charge obtained for the cathodic peak (at -0.2 V) is larger than the charge corresponding to the oxidation peak (at -0.13). The most plausible explanation for this discrepancy is that this is due to the overlap between the currents associated to the iron reduction and the HER and that rate of HER depends on the oxidation state of Fe. In this case, the base line for the integration would be unclear. For that reason, we only used the charge of the iron oxidation integrated from the anodic peak for the coulometric analysis that follows.

	Cathodic peak (μC/cm^2)	Anodic peak (μC/cm^2)
35 s in $Fe(ClO_4)_2$	184	63.5
60 s in $Fe(ClO_4)_2$	328	112
3 min in $Fe(ClO_4)_2$	432	181

Table 2. Involved charge under the peaks associated to the reduction and oxidation of the adsorbed iron species at -0.2 V and -0.13 V for each iron coverage.

Assuming that the dependence of the hydrogen charge (q_H) with the iron coverage can be expressed as:

$$q_H = q_H^{total}(1 - m\theta_{Fe}) \quad (1)$$

where q_H^{total} is the hydrogen charge on the blank experiment in the absence of iron (136 μC/cm^2), *m* is the number of Pt atoms blocked by each iron adatom and θ_{Fe} is the iron coverage (expressed as the number of iron adatoms per platinum atom). The latter can be related to the charge associated to the oxidation of iron 0 to iron *n* ($q_{Fe}^{Ox(0\rightarrow n)}$) under the peak at -0.13 V, as follows:

$$\theta_{Fe} = \frac{q_{Fe}^{Ox(0\rightarrow n)}}{q_{111}\, n\, x} \tag{2}$$

where *n* is the number of electrons involved in the oxidation process, and q_{111} is the charge corresponding to one electron per Pt atom on the Pt(111) surface (240 μC/cm^2). An extra parameter, *x*, is included to account for the formation of multilayers. Combining the equations 1 and 2 we can obtain the relationship between the hydrogen charge for each iron coverage (q_H) and the charge associated to the oxidation of iron ($q_{Fe}^{Ox(0\rightarrow n)}$) at -0.13 V (equation 3).

$$q_H = q_H^{total} - \left(\frac{q_H^{total} m}{240\, n\, x}\right) q_{Fe}^{Ox(0\rightarrow n)} \tag{3}$$

Figure 9. shows the obtained experimental relationship between the hydrogen charge and the charge associated to the oxidation of iron integrated for the different iron coverages.

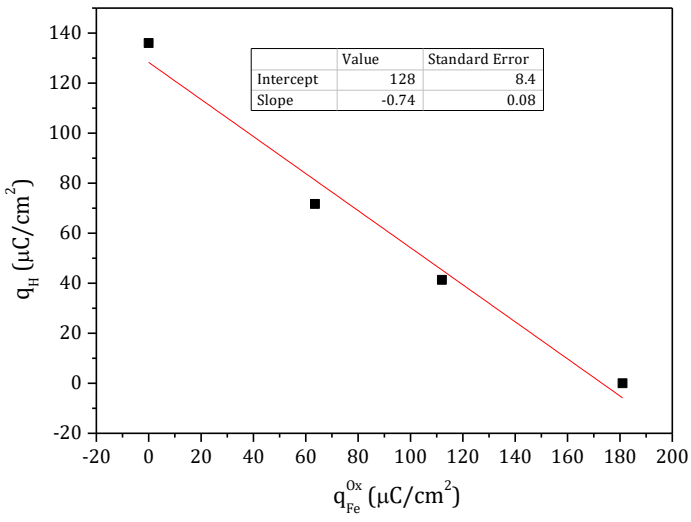

Figure 9. Plot of the hydrogen charge versus the iron charge at -0.13 V.

From the slope in Figure 9 the ratio between *m*, *n* and *x*, can be calculated resulting a value of $m/nx \approx 1.3$

In the same way, the iron charge and the hydrogen charge can be related with the resulting charge from the OH adsorption-desorption region, considering that this region contains two contributions: the OH on the free Pt(111) sites and on the iron species:

$$q_{OH}^{Fe} = q_{111}\theta_{Fe}\beta x \quad (4)$$

$$q_{OH}^{Pt} = q_{OH}^{blank}(1 - m\theta_{Fe}) \quad (5)$$

where β is the number of electrons involved for each iron adatom, i.e., the number of OH per iron atom added in this potential region. The total OH charge can be obtained by adding both equations 4 and 5. Combining the result with equations 1 and 2, the relation between the total charge in the OH region and the hydrogen charge (q_H) (eq 6) and the iron charge ($q_{Fe}^{Ox(0\rightarrow n)}$) (eq. 7) can be obtained, respectively.

$$q_{OH}^{Pt} + q_{OH}^{Fe} = \left(\frac{q_{OH}^{Blank}}{q_H^{total}} - \frac{q_{111}\beta x}{q_H^{total} m}\right) q_H + \frac{q_{111}\beta x}{m} \quad (6)$$

$$q_{OH}^{Pt} + q_{OH}^{Fe} = \left(\beta x - \frac{q_{OH}^{Blank} m}{q_{111}}\right) \frac{q_{Fe}^{Ox(0\rightarrow n)}}{n\,x} + q_{OH}^{Blank} \quad (7)$$

From the slopes or from the intercept shown in Figure 10A and 10B, it is concluded that $\beta x/m \approx 1.16$ and $\beta x - 0.64m \approx 0.74nx$ respectively. Combining both equations we get: $m/nx = 1{,}4$ in reasonable agreement with the value obtained from figure 9. Moreover, combining $\beta x/m \approx 1.16$ with $m/nx \approx 1.35$, we can obtain that $\beta \approx 1.6n$.

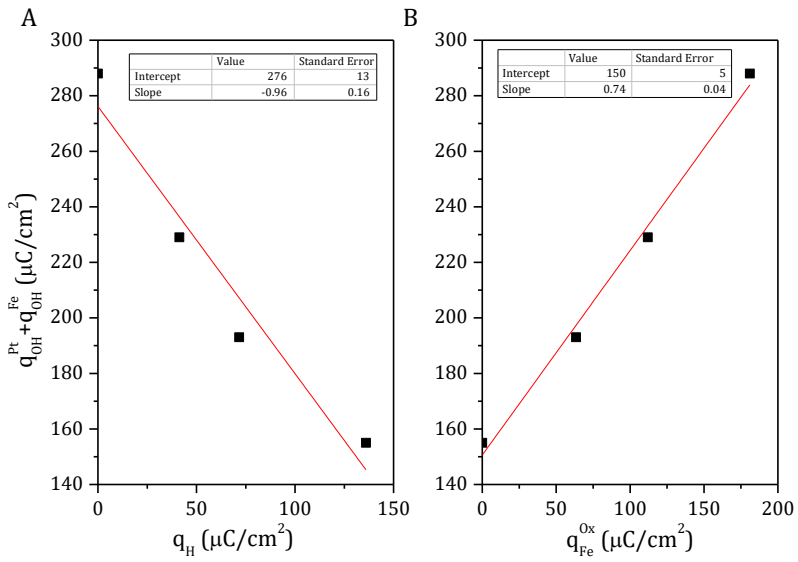

Figure 10. Relationship between the charge involved in the OH region versus hydrogen charge (A) and iron charge (B).

Since the obtained relations between m, β, n and x from the different plots are linearly dependent it is not possible to calculate the value for each parameter independently. However, given the irreversibility of the redox process in the OH region, the OH adsorption would lead to a formal change in the oxidation state of the adsorbed iron species. This change should be notable enough to accommodate a large part of the charge coming from the OH adsorption. Therefore, this would imply an oxidation state of the adsorbed iron not too high at potentials below 0.67 V. According to the coulometric analysis $\beta = 1.6n$, and hence, regardless of the possible values of the oxidation state either n=2 or n=2.7 reported in previous works, there is always an excess of adsorbed OH on the electrode surface. In this way, the corresponding values of β would range between 3 and 4. Since the maximum oxidation state of iron after the OH adsorption region would be the +3 state, the β value is higher than the number of electrons that the iron species can absorb. Even if the number of adlayers (x) were higher than one, there would be an excess of charge for each iron adatom in the first and the second adlayer. However, it is more reasonable to suppose that x=1, in which case the excess of OH charge should be accommodated on Pt sites close to the edges of the adsorbed iron. Therefore, the charge distribution in the OH region could not be regulated by steric effects. In this case, the electronic effects determine the distribution of OH species due to the large oxophilicity of iron.

In this regard, if n= 2.7 the adsorbed iron would undergo a small change in its oxidation state (from +2.7 to +3) leading to an excess of charge too high associated to the adsorbed OH on the iron species-Pt(111) edges. However, for a n value close to 2, $\beta \approx 3$ and hence, there would be only two extra electrons ascribed to two extra OH adsorbed on the edges. We consider this second interpretation the most plausible and therefore, we propose that the iron species adsorbed on the Pt(111) surface between -0.2 V and 0.67 V is $Fe(OH)_2$. This species would be forming a monolayer with ratio Pt/Fe m=2.6, and would be oxidized to Fe +3 at 0.67 V according to the reaction $Fe(OH)_2 + OH^- \rightarrow FeOOH + H_2O + e$.

2.3 Laser induced T-jump experiments

Laser induced temperature jump technique was employed in order to study the electric field on the Pt(111) surface modified with different iron coverages as possible descriptor for the HER. This technique provides information about the structure of the interfacial water network which is closely related with the electric field on the electrode surface.[17] In this regard, the water network adlayer is more disordered when the interfacial electric field is weaker, or similarly, when the applied potential is close to the potential of zero free charge (pzfc)/potential of maximum entropy (pme).[18] Previous reports proposed that a low energy of reorganization of the interfacial water as a consequence of a weak electric field, leads to a less ordered water network, and hence, this allows an easier transport of proton or OH^- through the double layer (for acid or alkaline media respectively) enhancing in this way the catalytic activity for the HER.[9-10] This idea was developed on the basis of the observation of higher rates of HER in acid media where the pzfc/pme of Pt(111) is closer to the onset of the reaction. Also, the experimental results for Pt(111) modified with nickel in alkaline media reinforce this hypothesis, since higher rates of HER seem again related with a shift of the pme toward negative potentials after Ni modification. For this reason, it is important to study a different system such as iron, apparently similar to nickel, in order to know better the effect of the interfacial electric field on the HER rate.

Figure 11 shows the laser transients for different iron coverages. For the lower coverage (Figure 11A), two transients close to zero (at 0.66 V a small bipolar contribution instead of a zero transient can be taken as a signal for the location of the pme) are observed at 0.06 V and 0.66 V. Between them, the laser transients are negative, suggesting the

existence of a negative electric field at the interface where the water molecules are oriented with their hydrogen atoms pointing toward the surface electrode. On the one hand, above 0.66 V, the transient changes sign becoming positive, indicating the presence of a positive electric field which orientate the oxygen of the water molecules toward the surface. The bipolar transient at 0.66 V for the lowest iron coverage appears located at potentials slightly lower than those observed for bare Pt(111) (~0.69 V) in previous reports[19] in the potential region where the OH adsorption take places. This agrees with the cyclic voltammograms showed in Figure 1 where the OH adsorption on the Pt(111) surface modified with iron takes place at lower potentials than for the free electrode. It is worth to highlight that according to previous works, the pme of Pt(111) keep invariable with the pH (300 mV vs SHE) in moderately acid solutions. Also, values of pzfc in alkaline solutions can be obtained by extrapolation of charge vs potential curves above the OH adsorption region. With this extrapolation procedure, it was shown that the pzfc remains invariable in the SHE scale in the whole pH range between 1 and 13.[20] However, laser induced potential transient in alkaline media show an inversion at much lower potentials, coinciding with the onset of OH adsorption. In this regard, such change of the sign of the transient could be due to a screening of the positive charge on the metal by the adsorbed OH species retaining part of their negative charge.[21] In this potential region dominated by the OH adsorption, the signal transients are similar for Pt(111) with and without iron showing a monotonic decay typical of the capacitive response of the double layer.[19] On the other hand, at potentials below 0.06 V surprisingly the laser transients become positive (explained below).

For the lowest iron coverages, the negative laser transients recorded below 0.66 V show lower intensity when compared with those obtained with the free Pt (111). However, as the iron coverage increases, the transients start inverting their sign becoming completely positive for the highest coverage (Figure 11D) except at the potentials 0.45 V and 0.55 V. During this process, as the iron amount increases on the electrode surface, three differentiated potential regions delimited by different bipolar or zero transients can be observed. These potential regions can be more easily observed in Figure 12A.

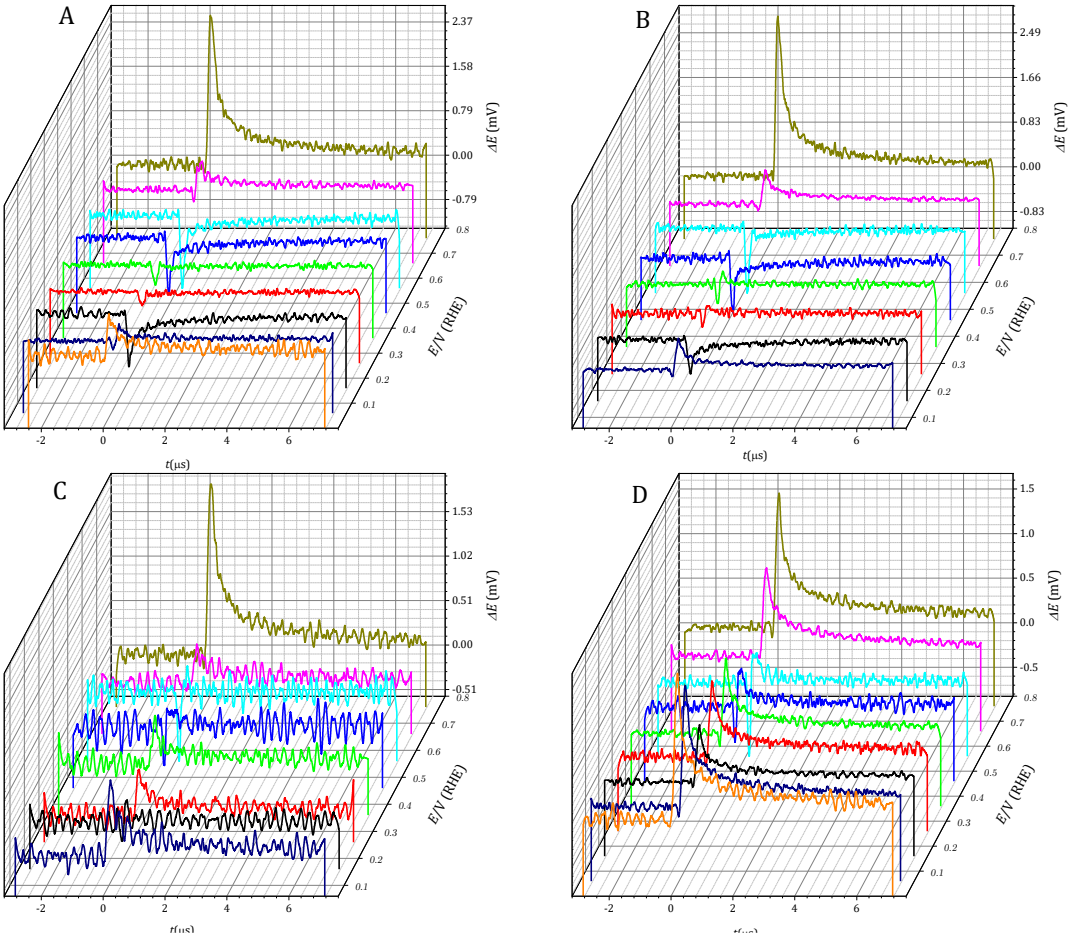

Figure 11. Laser ΔE vs t transients recorded on the Pt(111) surface modified with different coverages of $Fe(OH)_2$: <0.09 (A), <0.09 (B), 0.20 (C) and 0.40 (D). Laser beam energy: 0.8 mJ. Supporting electrolyte: 0.1 M NaOH

Figure 12A shows the maximum potential shift recorded in each transient at each potential taken from Figure 11. For bipolar transients, positive and negative peak values are plotted, and the middle point has been marked as a qualitative representation of the magnitude of the transient. At low potentials, the first inversion from positive to negative is shifted toward more positive potential from 0.06 V to 0.16 V as iron coverage increases. For the highest coverage, there is no inversion and the transients are positive in the whole potential region. Close to the onset of the hydrogen adsorption the intensity of the negative transients decreases and become almost zero at 0.26 V and 0.36 V for the two lowest iron coverages. For the highest iron coverage, the transients remain positive in the hydrogen and double layer region but decrease intensity as the potential approaches the OH adsorption region. On the other side, the zero transient appearing at 0.69 V for the

blank is shifted to less positive potentials as iron amount increases until it almost overlaps with the transients in the doble layer. The drop of the negative electric field as iron amount increases suggests that the water molecules network presents a less rigid structure in the double layer region. However, below 0.16 V ΔE_{peak} shows a positive trend while the potential is less positive such as it is mentioned above.

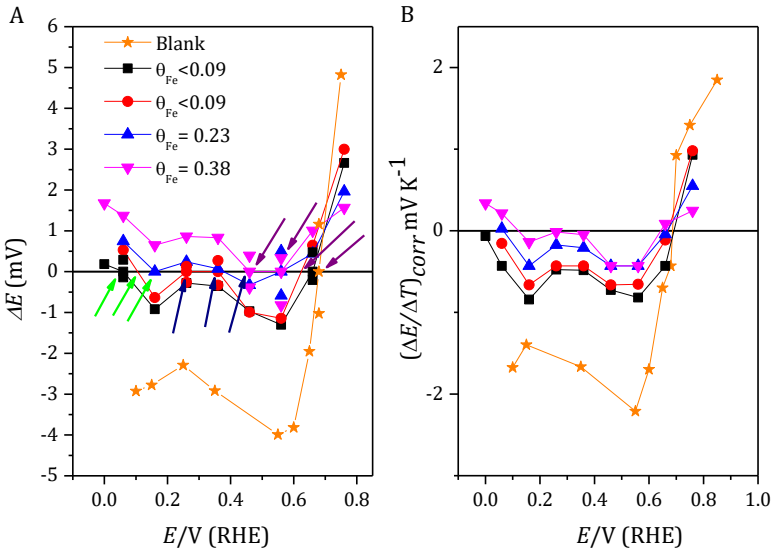

Figure 12. ΔE_{peak} corresponding to each transient peak vs E for each iron coverage. In case of the bipolar transient the value of zero has been given to ΔE, around which the peak potential is shown for each positive and negative contribution (A). Plot of the thermal coefficients for each applied potential for the Pt(111) modified with different iron coverages (B). The corresponding values to blank are taken from previous reports.

Figure 12A allows a qualitative visualization of the evolution of the magnitude of the transients for each iron coverage with the applied potential. However, a more quantitative analysis leads to the calculation of the values of the thermal coefficient, $(\partial \Delta E/\partial T)$, as dicussed below. Such values are plotted in Figure 12B and give a more accurate representation of the interfacial electric field. As it has been explained in detail elsewhere[17a], it is possible to perform a more quantitative analysis of the laser transients by considering the theoretical relation between the potential difference (ΔE) in the interface and the temperature relaxation (ΔT) obtained by a model of heat transfer for measuring times sufficiently longer that the duration of the laser pulse:

$$\Delta E = \frac{1}{2}\left(\frac{\partial E}{\partial T}\right)\Delta T_0\sqrt{\frac{t_0}{t}} \quad (8)$$

Where t_0 is the duration of the laser pulse (5 ns) and ΔT_0 is the maximum temperature change (~27 K for this work) which can be obtained by a model heat diffusion where the parameters reflectivity, thermal diffusivity and thermal conductivity of the metal and the solution are required.[17a] In this way, it is possible to obtain the thermal coefficients of the double layer formation, $(\partial E/\partial T)$, by plotting ΔE vs $t^{-1/2}$ such as it has been already explained in previous works. However, this result is uncertain when the potential transient is not monotonous, namely, around the pme. Still, the good coincidence in the trends represented in Figure 12A and B, give confidence in this analysis. Figure 12B plots the thermal coefficients $\left(\frac{\partial E}{\partial T}\right)$ obtained for each applied potential. Taking into account the thermosdiffusion effect as consequence of the difference of temperature between the reference and the working electrode, 0.43 mV K^{-1} has been subtracted for each plotted thermal coefficient. This value was calculated from the mobility and the Eastman entropies of transport of the ions for a 0.1M NaOH solution.[22] As can be seen in Figure 12B, in the OH region $\left(\frac{\partial E}{\partial T}\right) = 0$ is shifted toward less positive values as iron coverage increases. However, in the hydrogen adsorption-desorption region $\frac{\partial E}{\partial T} = 0$ is placed at less positive potential as iron amount increases. In this last case, the trend to diminish the negative electric field even becoming positive as the applied potential is more negative would suggest an effect of the HER itself. One possibility to explain this behavior would be to consider that, since the first step in the HER in alkaline media is the hydrogen adsorption from the water molecule, when they approach the surface, the high oxyphilic capacity of the iron lead to the inversion of the orientation of the water molecules originating a rigid network with their hydrogen atoms pointing to the solution, and hence screening the superficial electric field. Therefore, when the potential is more negative there is a larger amount of water molecules inverted on the surface electrode inducing a greater negative dipolar contribution.

Another possible explanation would be that the presence of a rigid OH network of the $Fe(OH)_2$, favoured by the iron oxophilicity, with their hydrogen atoms pointed toward the solution favours the hydrogen bonding of the solvent molecules with the oxygen towards the surface, leading again to a negative dipolar contribution. In this case, the

more negative the potential the larger the positive hydrogen dipole, increasing the polarization of the hydrogen bonded water layer.

In this regard, Figure 12 shows that the interfacial electric field is closer to zero in the region near to the equilibrium potential of the HER for the lowest iron coverage. Therefore, this weak electric field closer the onset of the HER could provide a lower energy of reorganization of the interfacial water facilitating the charge transfer through the double layer and hence, enhancing the catalytic activity for the HER. This could explain the decrease of the overpotential associated to the onset of the HER observed in Figure 7 as the iron coverage decreases. In this regards, it is worth noting that recent spectroscopic measurements on thin Pd layers on Au electrodes led to the conclusion that a more ordered ice-like structure is correlated with a higher activity for hydrogen evolution [23]. This observation contrasts with the conclusion reached in the present paper and calls for a more extensive investigation of the role of the multiple factors that can influence the rate of hydrogen evolution. It is clear that not one single descriptor is sufficient to explain the trends observed between different materials and conditions for the activity towards the HER, but an interplay of multiple factors must be taken into account. Moreover, the reduction of the iron to the zero-valence state would disrupt the above described scenarios changing the catalytic activity. Most likely the iron adatoms will bear a positive partial charge, increasing the polarization of the water with the oxygen pointing towards surface.

4 Conclusion

An interfacial study has been carried out for the Pt(111) surface modified with iron adatoms in alkaline media. The results obtained with cyclic voltammetry suggest the presence of the $Fe(OH)_2$ species adsorbed on the surface electrode with a relationship Pt/Fe m=2.6. This iron hydroxide is oxidized to FeOOH at 0.66 V approximately and reduced to Fe^0 below -0.2 V. Different $Fe(OH)_2$ coverages were prepared and their effect on the HER was investigated. In this regard a decrease of the HER rate was observed as the iron coverages was increased.

To obtain information about the interfacial electric field the laser-induced temperature-jump technique was employed. The results showed a progressive inversion of the electric field with increasing iron coverage. On the other side, at low potentials, the iron presence

decreases the negative electric field, even turning it into positive values. Specifically, for the lowest iron coverage the interfacial electric field reaches a value close the equilibrium potential of the HER. Therefore, the less rigid water structure facilitates the charge transfer though the double layer, and hence enhances the rate of HER. However, the discrepancy between this interpretation and recent spectroscopic results[23] calls for more work to further understand the interplay of the different factors that can affect the structure of interfacial water and, consequently, the activity for the HER.

Acknowledgements

This research was funded by Ministerio de Ciencia e Innovación (Spain) grant number PID2019-105653GB-I00 and Generalitat Valenciana (Spain) grant number PROMETEO/2020/063

References

1. (a) Gileadi, E., *Physical Electrochemistry: Fundamentals, Techniques and Applications*. WILEY-VCH Verlag GmbH & Co: 2011; (b) Conway, B. E.; Gileadi, E., Kinetic Theory of pseudo-capacitance and electrode reactions at appreciable surface coverage. *J. Chem. Soc., Faraday Trans.* **1962**, 2493-2509; (c) Diaz-Morales, O.; Calle-Vallejo, F.; de Munck, C.; Koper, M. T. M., Electrochemical water splitting by gold: evidence for an oxide decomposition mechanism. *Chemical Science* **2013,** *4*, 2334-2343.

2. Bockris, J. O. M., The origin of ideas on a Hydrogen Economy and its solution to the decay of the environment. *International Journal of Hydrogen Energy* **2002,** *27* (7-8), 731-740.

3. Jaramillo, T. F., Identification of active edge sites for electrochemical H2 evolution from MoS2 nanocatalysts. *Science* **2007,** *317*.

4. (a) Lasia, A.; Rami, A., Kinetics of hydrogen evolution on nickel electrodes. *Journal of Electroanalytical Chemistry* **1990,** *294*, 123-141; (b) Birry, L.; Lasia, A., Studies of the hydrogen evolution reaction on Raney nickel—molybdenum electrodes. *Journal of Applied Electrochemistry* **2004,** *34*, 735-749.

5. (a) Trasatti, S., Work function, electronegativity, and electrochemical behavior of metals.3. Electrolytic hydrogen evolution in acid solutions. *Journal of Electroanalytical Chemistry* **1972,** *39*; (b) Nørskov, J. K., Trends in the exchange current for hydrogen evolution. *Journal of the Electrochemical Society* **2005,** *152*; (c) Sheng, W.; Myint, M.; Chen, J. G.; Yan, Y., Correlating the hydrogen evolution reaction activity in alkaline electrolytes with the hydrogen binding energy on monometallic surfaces. *Energy & Environmental Science* **2013,** *6*, 1509-1512.

6. Zeradjanin, A. R.; Vimalanandan, A.; Polymeros, G.; Topalov, A. A.; Mayrhofer, K. J. J.; Rohwerder, M., Balanced Work Function as a Driver for Facile Hydrogen Evolution Reaction – Comprehension and Experimental Assessment of Interfacial Catalytic Descriptor. *Physical Chemistry Chemical Physics* **2017,** *19*, 17019-17027.

7. (a) Subbaraman, R.; Dusan, T.; Strmcnik, D.; Chuang, K.-C.; Masanobu, U.; Paulikas, A. P.; Stamenkovic, V.; Markovic, N. M., Enhancing Hydrogen Evolution Activity in Water Splitting by Tailoring Li^+-$Ni(OH)_2$-Pt Interfaces. *Science* **2011,** *334* (6060), 1256-1260; (b) Chen, X.; McCrum, I. T.; Schwarz, K.; Janik, M. J.; Koper, M. T. M., Co-adsorption of cations as the cause of the apparent pH dependence of hydrogen adsorption on a stepped platinum single-crystal electrode. *Angewandte Chemie - International Edition* **2017,** *56*, 15025-15029.
8. Subbaraman, R.; Tripkovic, D.; Chang, K. C.; Strmcnik, D.; Paulikas, A. P.; Hirunsit, P.; Chan, M.; Greeley, J.; Stamenkovic, V.; Markovic, N. M., Trends in activity for the water electrolyser reactions on 3d M(Ni,Co,Fe,Mn) hydr(oxy)oxide catalysts. *Nat. Mater.* **2012,** *11* (6), 550-557.
9. Ledezma-Yanez, I.; Wallace, W. D. Z.; Sebastián-Pascual, P.; Climent, V.; Feliu, J. M.; Koper, M. T. M., Interfacial water reorganization as a pH-dependent descriptor of the hydrogen evolution rate on platinum electrodes. *Nature Energy* **2017,** *2* (4), 17031-17037.
10. Sarabia, F. J.; Sebastian-Pascual, P.; Koper, M.; Climent, V.; Feliu, J. M., Effect of interfacial water structure on the Hydrogen evolution Reaction on Pt(111) modified with different Nickel Hydroxide coverages in alkaline media. *ACS Applied Materials & Interfaces* **2018**, 10.1021/acsami.8b15003.
11. Clavilier, J.; Armand, D.; Sun, S. G.; Petit, M., Electrochemical adsorption behaviour of platinum stepped surfaces in sulphuric acid solutions *J. Electroanal. Chem.* **1986,** *205* (1-2), 267-277.
12. Korzeniewski, C.; Climent, V.; Feliu, J. M., Electrochemistry at Platinum Single Crystal Electrodes. In *Electroanalytical Chemistry: A Series of Advances*, Bard, A. J.; Zoski, C., Eds. CRC Press: Boca Raton, 2012; Vol. 24, pp 75-169.
13. Pourbaix, M., *Atlas of Electrochemical Equilibria in Aqueous Solutions*. Second English Edition ed.; Pourbaix, M.: Houston, 1974; p 644.
14. Weaver, M. J., Potentials of zero charge for platinum(111)-aqueous interfaces: A combined assessment from in-situ and ultrahigh-vacuum measurements. *Langmuir* **1998,** *14* (14), 3932-3936.
15. Seto, K.; Iannelli, A.; Love, B.; Lipkowski, J., The influence of surface crystallography on the rate of hydrogen evolution at Pt electrodes. *Journal of Electroanalytical Chemistry and Interfacial Electrochemistry* **1987,** *226* (1-2), 351-360.
16. Shinagawa, T.; Garcia-Esparza, A. T.; Takanabe, K., Insight on Tafel slopes from a microkinetic analysis of aqueous electrocatalysis for energy conversion. *SCIENTIFIC REPORTS* **2015,** *5*, 13801.
17. (a) Garcia-Araez, N.; Climent, V.; Feliu, J. M., Temperature Effects on Platinum Single-Crystal/Aqueous Solution Interphases. Combining Gibbs Thermodynamics with Laser-Pulsed Experiments. *Interfacial Phenomena in Electrocatalysis* **2011,** *51*, 1-105; (b) Climent, V.; Coles, B. A.; Compton, R. G., Laser-induced potential transients on a Au(111) single-crystal electrode. Determination of the potential of maximum entropy of double layer formation. *J. Phys. Chem. B* **2002,** *106*, 5258-5265; (c) Climent, V.; Coles, B. A.; Compton, R. G., Coulostatic Potential Transients Induced by Laser Heating of a Pt(111) Single-Crystal Electrode in Aqueous Acid Solutions. Rate of Hydrogen Asorption and Potential of Maximum Entropy. *J. Phys. Chem. B* **2002,** *106*, 5988-5996.

18. Garcia-Araez, N.; Climent, V.; Feliu, J. M., Evidence of water reorientation on model electrocatalytic surfaces from nanosecond-laser-pulsed experiments. *J. Am. Chem. Soc.* **2008,** *130* (12), 3824-3833.
19. Sarabia, F. J.; Sebastián, P.; Climent, V.; Feliu, J. M., New insights into the Pt(hkl)-alkaline solution interphases from the laser induced temperature jump method. *Journal of Electroanalytical Chemistry* **2020,** *872*, 114068.
20. Rizo, R.; Sitta, E.; Herrero, E.; Climent, V.; Feliu, J. M., Towards the understanding of the interfacial pH scale at Pt(111) electrodes. *Electrochim. Acta* **2015,** *162*, 138-145.
21. Huang, J.; Malek, A.; Zhang, J.; Eikerling, M. H., Non-monotonic Surface Charging Behavior of Platinum: A Paradigm Change. *The Journal of PHYSICAL CHEMISTRY C* **2016,** *120* (25), 13587-13595.
22. Agar, J. N., Thermogalvanic cells. Wiley-Interscience: New York, 1963; Vol. 3, pp 31-121.
23. (a) Zhang, Y.-J.; Su, Z.-F.; Li, J.-F.; Lipkowski, J., Water structure at the multilayers of palladium deposited at nanostructured Au electrodes. *J. Electroanal. Chem.* **2021,** *896*, 115243; (b) Wang, Y.-H.; Zheng, S.; Yang, W.-M.; Zhou, R.-Y.; He, Q.-F.; Radjenovic, P.; Dong, J.-C.; Li, S.; Zheng, J.; Yang, Z.-L.; Attard, G.; Pan, F.; Tian, Z.-Q.; Li, J.-F., In situ Raman spectroscopy reveals the structure and dissociation of interfacial water. *Nature* **2021,** *600* (7887), 81-85.